

# Matched-Filter and Stochastic-Simulation-Based Methods of Gust Loads Prediction

Robert C. Scott\*

*NASA Langley Research Center, Hampton, Virginia 23681-0001*

Anthony S. Pototsky†

*Lockheed Engineering and Sciences Company, Inc., Hampton, Virginia 23666-1339*

and

Boyd Perry III‡

*NASA Langley Research Center, Hampton, Virginia 23681-0001*

Two analysis methods, one deterministic and the other stochastic, for computing maximized and time-correlated gust loads for aircraft with nonlinear control systems are described. The first method is based on matched-filter theory, and the second is based on stochastic simulation. This article summarizes the methods, discusses the selection of gust intensity for each method, and presents numerical results. The critical gust profiles and the maximized and time-correlated load time histories obtained from the two methods are compared. Their striking similarity demonstrates that the key quantities from the matched-filter-based method are realized in the stochastic-simulation-based method. The similarity between the results of the two methods is seen to exist for both linear and nonlinear configurations, indicating that these methods are capable of predicting the critical gust profiles and loads for those classes of nonlinear systems examined.

## Nomenclature

$\bar{y}$	= ratio of rms value of response $y$ to rms value of turbulence
$k$	= impulse strength
$L$	= scale of turbulence, ft
$s$	= Laplace variable
$T$	= total length of simulation used in the stochastic-simulation-based method, s
$t$	= time, s
$t_0$	= time shift used in matched-filter-based methods, s
$U_o$	= design gust velocity, ft/s
$V$	= airspeed, ft/s
$y(t)$	= time response of output quantity $y$
$y_{\text{design}}$	= design value of output quantity $y$
$y_{\text{max}}$	= maximum value of $y(t)$
$z(t)$	= time response of output quantity $z$
$\delta(t)$	= impulse time history
$\delta_{\text{rudder}}$	= rudder deflection commanded by control system
$\eta$	= white noise
$\eta_d$	= ratio of peak value to design value of output quantity
$\sigma_g$	= rms value of gust velocity, ft/s
$\tau_0$	= time span of extracted time histories in the stochastic-simulation-based method, s

Presented as Paper 93-1365 at the AIAA 34th Structures, Structural Dynamics, and Materials Conference, La Jolla, CA, April 28–30, 1993; received Jan. 23, 1994; revision received March 27, 1995; accepted for publication March 28, 1995. Copyright © 1995 by the American Institute of Aeronautics and Astronautics, Inc. No copyright is asserted in the United States under Title 17, U.S. Code. The U.S. Government has a royalty-free license to exercise all rights under the copyright claimed herein for Governmental purposes. All other rights are reserved by the copyright owner.

\*Research Engineer, Aeroelasticity Branch, M/S 340, Structures Division. Member AIAA.

†Staff Engineer, 144 Research Drive. Senior Member AIAA.

‡Assistant Branch Head, Aeroelasticity Branch, M/S 340, Structures Division.

## Introduction

FOR several years NASA Langley Research Center has conducted research in the area of time-correlated gust loads and published a number of papers on the subject.<sup>1–5</sup> The initial research was restricted to mathematically linear systems.<sup>1–3</sup> Recently, however, the focus of the research has been on defining methods that will compute design gust loads for an aircraft with a nonlinear control system.<sup>4,5</sup> To date, two such methods have been defined: one is based on matched filter theory and the other is based on stochastic simulation.

The matched-filter-based (MFB) method was developed first and was reported on in Ref. 4. The MFB method employs optimization to solve for its answers and this method comes in two varieties: the first uses a one-dimensional search procedure; the second a multidimensional search procedure. Based on preliminary results, the first is significantly faster to run and gives design loads only slightly lower in magnitude than the second.

The stochastic-simulation-based (SSB) method has evolved over the past several years. The SSB method was first reported on in 1992 (Ref. 5), and since then an improvement in the method has been made. The improvement involves what is referred to in the SSB method as the extraction and averaging procedure. This procedure has been made to be independent of answers from the MFB method.

The purpose of this article is to present numerical results recently obtained by applying these two methods. The mathematical model is a model of a current transport aircraft equipped with a nonlinear yaw damper. The model has the same level of complexity as those commonly used in the aircraft industry.

## Description of Methods

This section presents brief descriptions of two analysis methods for computing maximized and time-correlated gust loads for linear and nonlinear airplanes. The first method is the MFB method; the second, the SSB method.

### MFB Method

The MFB method is implemented one way for a linear aircraft and two possible ways for a nonlinear aircraft.

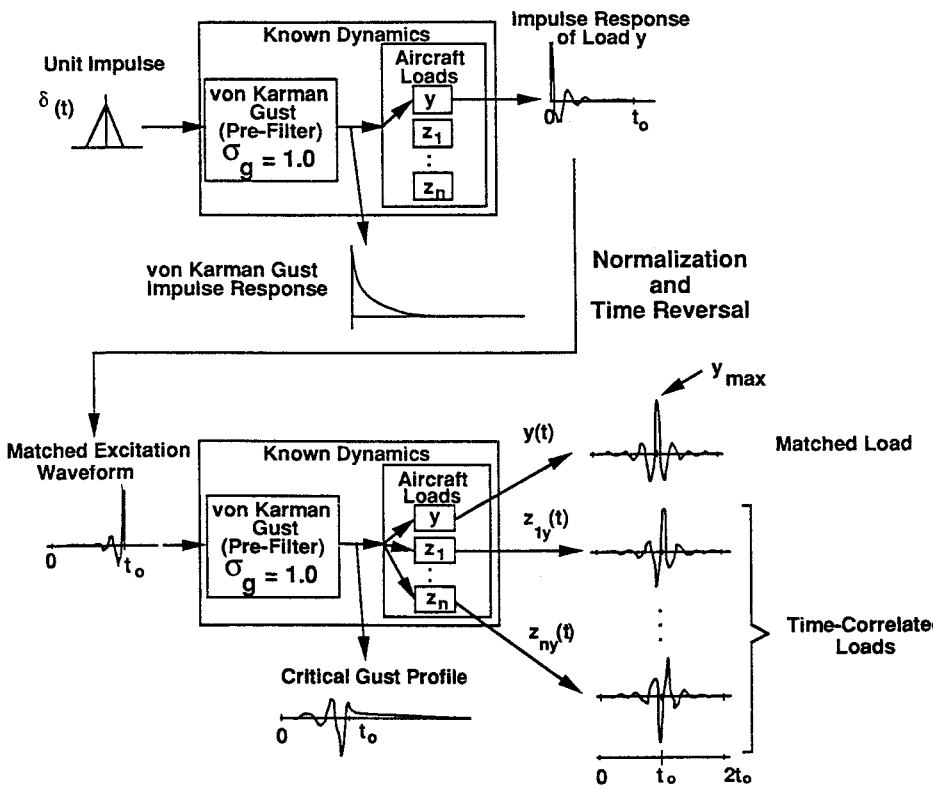


Fig. 1 Schematic of the MFB linear method.

#### Implementation for Linear Airplane

A detailed theoretical development of the MFB method for linear systems can be found in Ref. 2. The signal flow diagram in Fig. 1 outlines the implementation and illustrates the intermediate and final products of the process.

Transfer-function representations of atmospheric turbulence and aircraft loads are combined in series and represent the "known dynamics" boxes in the figure. A transfer-function representation of the von Kármán spectrum is chosen for the gust filter. Load  $y$  is the load to be maximized. Loads  $z_1 - z_n$  are the loads to be time correlated with load  $y$ . There are three major steps in the process:

*Step 1:* application of an impulse function of unit strength to the combined linear system, producing the impulse response of load  $y$ . Based on the time required for the load impulse responses to damp out, a value of  $t_0$  is selected. Too large a value will unduly increase the amount of computations required; too small a value will not give accurate answers.

*Step 2:* the normalization of this impulse response by its own energy, followed by its reversal in time. As shown in Fig. 1 time reversal is the name for the procedure where the impulse response is rearranged such that the maximum value occurs at a time  $t_0$  and the minimum value occurs at time zero.

*Step 3:* the application of this normalized reversed signal to the combined linear system, producing time histories of load  $y$  and time histories of loads  $z_1 - z_n$ . Within the time history of load  $y$ , the maximum value is  $y_{\max}$ . Theory guarantees that there is no other normalized signal that, when applied to the combined linear system, will produce a value of  $y$  larger than  $y_{\max}$ . This guarantee is a fundamental result of the MFB linear method.

For simplicity of discussion throughout this article, these three steps will be referred to as the "MFB linear method."

#### Implementation for Nonlinear Airplane—One-Dimensional Search Procedure

A detailed development of the MFB methods for a nonlinear airplane can be found in Ref. 4. Figure 2 contains a signal flow diagram of the two possible implementations. Although

very similar to Fig. 1, Fig. 2 contains some important differences that are indicated by the shaded boxes, quotation marks, and dashed lines.

In Fig. 2 the initial impulse may have a nonunity strength; the aircraft loads portion of the known dynamics box contains nonlinearities; and the shape of the excitation waveform and the value of  $y_{\max}$  are functions of the initial impulse strength. In addition, the matched excitation waveform and the matched load are shown in quotes because, for nonlinear systems, there is no guarantee that  $y_{\max}$  is a global maximum.

The application of the one-dimensional search procedure is as follows:

*Step 1:* select a value of  $\sigma_g$ .

*Step 2:* select a range of values of impulse strength  $k$ .

*Step 3:* perform steps 1–3 of the MFB linear method for each value of  $k$ , obtaining values of  $y_{\max}$  and corresponding matched excitation waveforms.

*Step 4:* from these values of  $y_{\max}$ , select the maximum value of  $y_{\max}$  and its corresponding matched excitation waveform and corresponding impulse strength.

#### Implementation for Nonlinear Airplane—Multidimensional Search Procedure

The multidimensional search procedure uses as its starting point the matched excitation waveform from step 4 of the one-dimensional search procedure. In an attempt to obtain an even larger value of  $y_{\max}$ , a constrained optimization scheme alters the shape, but not the energy of the excitation waveform. The waveform is represented by a linear combination of Chebyshev polynomials. The coefficients of the polynomials are the design variables used in the optimization procedure. The converged value of  $y_{\max}$  is greater than or equal to the  $y_{\max}$  obtained from the one-dimensional search. The dashed line in the figure illustrates the optimization loop.

#### SSB Method

The SSB method is implemented the same way for both linear and nonlinear airplanes. Figure 3 outlines the implementation. There are four major steps in the process:

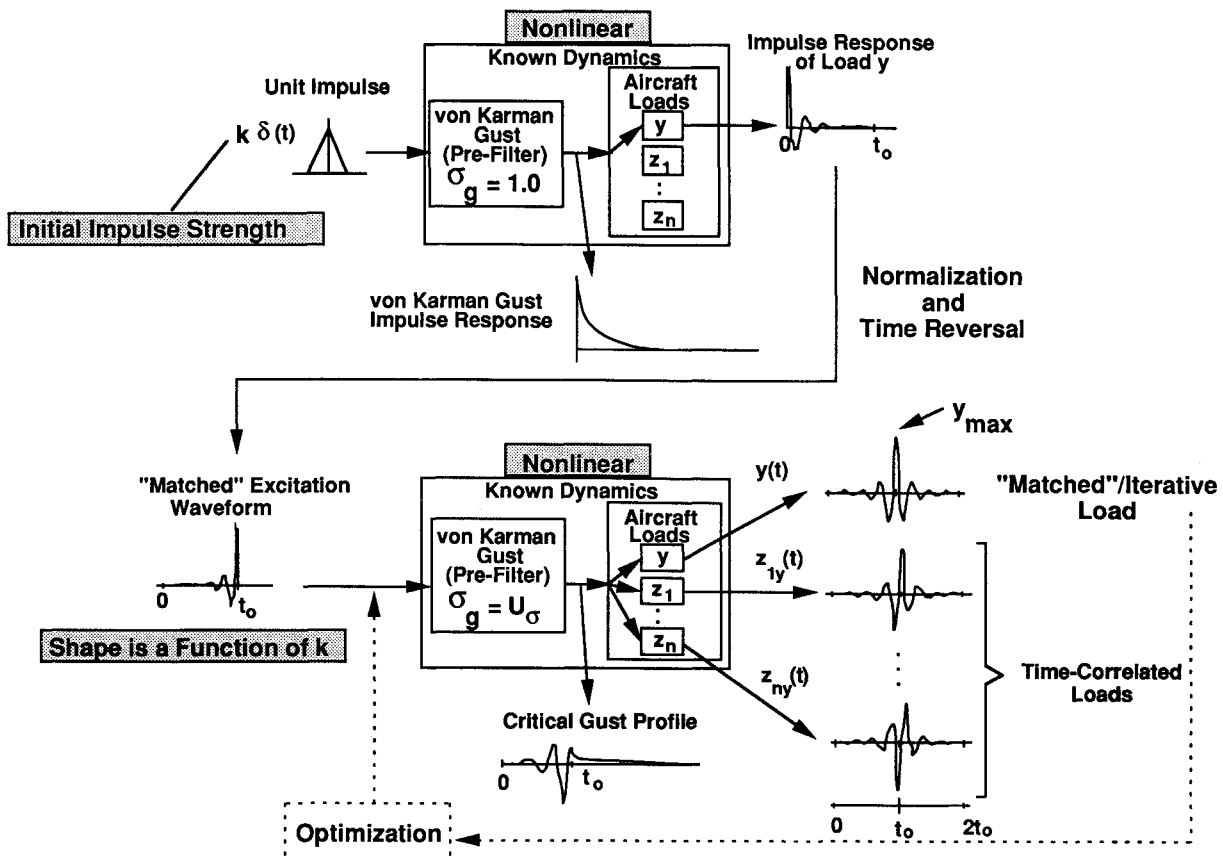


Fig. 2 Schematic of the MFB one-dimensional and multidimensional searches.

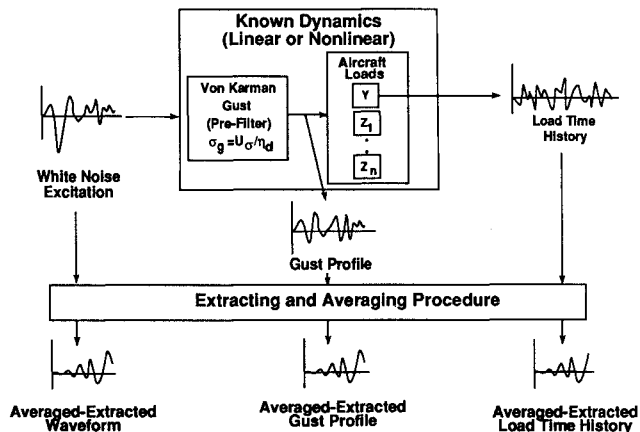


Fig. 3 Schematic of the SSB method.

*Step 1:* a value of  $\sigma_g$  is selected for the gust filter. Then an approximation to Gaussian white noise is applied to the gust filter producing a time history of stationary Gaussian atmospheric turbulence with a von Kármán power spectral density function. The turbulence time history is then applied, by simulation, to the aircraft model, producing a load time history.

*Step 2:* for each load output, a search of the time history of that load locates "points in time" where peak loads occur. Of these peaks, those that have the largest magnitude within a time span of  $\pm \tau_0$  s are identified for "extraction." In the extraction procedure,  $\pm \tau_0$  second's worth of all of the load time histories and  $\pm \tau_0$  second's worth of the corresponding gust time history, centered on the point in time where the peak occurred, are saved. Figure 4 shows the extraction procedure, where a load time history and the corresponding gust profile time history have been extracted. The effects of vary-

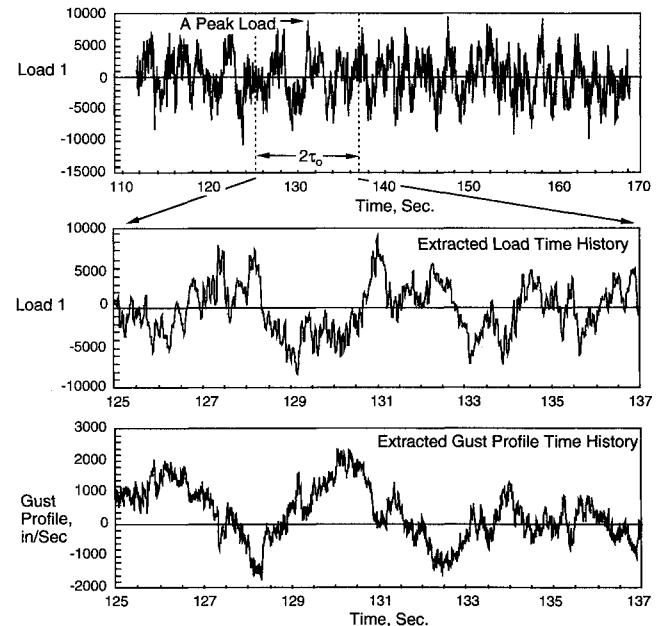


Fig. 4 Extraction procedure for SSB method.

ing  $\tau_0$  will be discussed in the Results and Discussion section of this article.

*Step 3:* the extracted load time histories and corresponding gust time histories are "lined up in time" so that each begins at a relative time of zero and each ends  $2\tau_0$  s later. Figure 5 shows 11 extracted gust and load time histories lined up in time and plotted together. At each point in time the quantities are averaged, producing "averaged-extracted" gust profiles and load time histories.

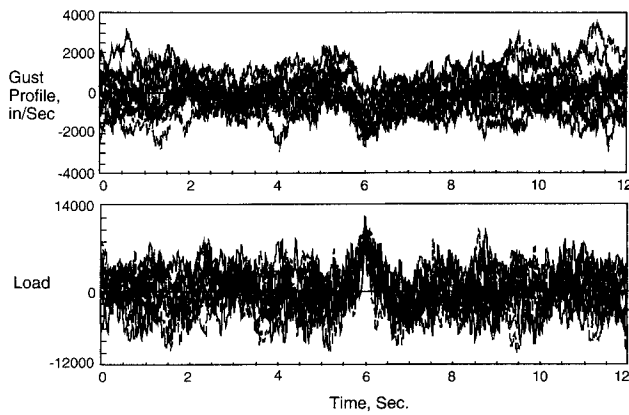


Fig. 5 Eleven extracted gust profiles and load time histories.

Step 4: calculate statistical quantities: level crossings, zero crossings, and rms values.

#### Selection of Gust Intensities

The MFB and SSB methods both employ the following transfer function approximation of the von Kármán power spectral density function<sup>6</sup>:

$$\frac{w_g}{\eta} = \sigma_g \sqrt{\frac{L}{\pi V}} \times \frac{[1 + 2.618(L/V)s][1 + 0.1298(L/V)s]}{[1 + 2.083(L/V)s][1 + 0.823(L/V)s][1 + 0.0898(L/V)s]} \quad (1)$$

This expression is referred to in this article as the gust filter, where the quantity  $\sigma_g$  is the intensity of the gust. In the power spectrum,  $\sigma_g$  is the standard deviation, which, assuming zero mean, is also equal to the rms value, of gust velocity. Both the MFB and the SSB methods use quantity  $\sigma_g$  as gust intensity. In order to compare the results from the MFB method with the results from the SSB method, it is necessary to properly select the gust intensity for each method.

The purpose of this section is to present the reasoning behind the selection of the values of  $\sigma_g$  for MFB and SSB methods, so that the results of the two methods may be compared. It will be shown that the gust intensities used for the two analyses differ by a factor of  $\eta_d$ .

#### Design Envelope Criterion

The following equation, from Ref. 7, expresses the "design value" of quantity  $y$  as defined in the design envelope criterion

$$y_{\text{design}} = \bar{A}_y U_\sigma \quad (2)$$

where the quantity  $\bar{A}_y$  is the rms value of quantity  $y$  per unit rms gust intensity, obtained from a conventional random process analysis of the airplane, and  $U_\sigma$  is specified in the criterion. Quantity  $y_{\text{design}}$  is interpreted as a peak value. From Ref. 7 the quantity  $U_\sigma$  in Eq. (2) is shown to be the product of the gust rms value and the design ratio of peak value of load to rms value of load, or

$$U_\sigma = \sigma_g \eta_d \quad (3)$$

Although the criterion specifies only the product of  $\sigma_g$  and  $\eta_d$  in Eq. (3), not each term separately, the breakdown is important in the selection of gust intensities for the SSB method and, therefore, in comparing MFB and SSB results.

#### MFB Gust Intensity

Reference 4 shows that, as a consequence of the normalization of the excitation waveform by its own energy and the

use of unity gust intensity, the quantity  $y_{\text{max}}$  from the MFB linear method is equal to the quantity  $\bar{A}_y$  from a conventional random process analysis, or

$$y_{\text{max}}(\sigma_g = 1) = \bar{A}_y \quad (4)$$

In Eq. (4)  $y_{\text{max}}$  is interpreted as an rms value, not a peak value. Substituting Eq. (4) into Eq. (2),  $y_{\text{design}}$  is now

$$y_{\text{design}} = y_{\text{max}}(\sigma_g = 1) U_\sigma \quad (5)$$

If, in performing the MFB linear method,  $U_\sigma$  is used for the gust intensity, then the quantity  $y_{\text{max}}$  is equal to

$$y_{\text{max}}(\sigma_g = U_\sigma) = \bar{A}_y U_\sigma \quad (6)$$

The right-hand sides of Eqs. (2) and (6) are seen to be equal, therefore,

$$y_{\text{design}} = y_{\text{max}}(\sigma_g = U_\sigma) \quad (7)$$

Two options for the value of  $\sigma_g$  have been offered:  $\sigma_g = 1$ , for which  $y_{\text{design}}$  is defined by Eq. (5); and  $\sigma_g = U_\sigma$ , for which  $y_{\text{design}}$  is defined by Eq. (7). When analyzing a linear system the choice of  $\sigma_g$  is irrelevant because the same value of  $y_{\text{design}}$  will be obtained in either case. However, when nonlinearities are introduced into aircraft control systems, loads are not linearly proportional to gust intensity. Consequently,  $\sigma_g$  should be set to  $U_\sigma$  in the MFB nonlinear calculations, or

$$\sigma_{g\text{MFB}} = U_\sigma \quad (8)$$

and the resulting " $y_{\text{max}}$ " values from the method should be interpreted as  $y_{\text{design}}$ .

#### SSB Gust Intensity

In the SSB method, because random inputs are applied to the simulation, the outputs are already "peaks" in the previous sense. Referring again to Eq. (3) and recalling that the breakdown between  $\sigma_g$  and  $\eta_d$  is not specified (only their product is specified), Eq. (3) can be rewritten for the SSB gust intensity:

$$\sigma_{g\text{SSB}} = U_\sigma / \eta_d \quad (9)$$

To use Eq. (9), the analyst must select a value for  $\eta_d$ . This approach was applied by Gould in his work with stochastic simulation<sup>8</sup> in which he used the value of 3 for  $\eta_d$ .

#### Mathematical Model

A mathematical model of a small two-engine jet transport equipped with a nonlinear yaw damper is used for all the calculations performed in this article. Figure 6 depicts the

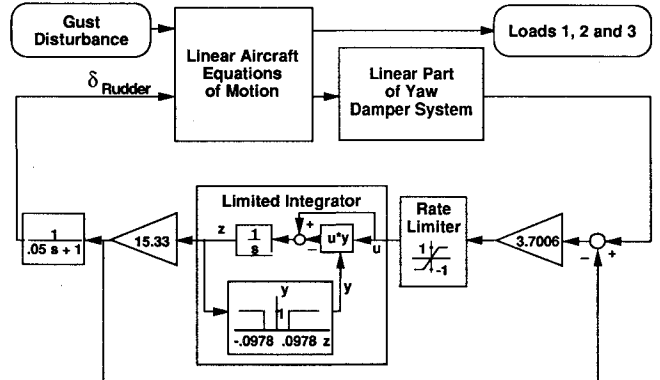


Fig. 6 Block diagram of transport model with nonlinear control system.

nonlinear math model in block diagram form. The portion of the math model that represents the airplane is linear and consists of 12 antisymmetric flexible modes and 3 rigid-body lateral-directional modes. A doublet-lattice code was used to calculate the unsteady aerodynamics for a Mach number of 0.85. These unsteady aerodynamic forces were converted to the *s* plane by evaluating the coefficients of a series proposed by Richardson.<sup>9</sup> An *s*-plane modeling technique was used to describe the lag states representing the gust penetration, and it consisted of two states. The basic aeroelastic equations of motion were composed of 75 states for a flight condition at an altitude of 28,000 ft. The yaw damper control system had two nonlinear elements: 1) a rate limiter and 2) a deflection limiter for the rudder. The structure of the yaw damper is shown in the figure. The yaw damper contributed nine additional states to the math model. The final state-space re-

alization had 86 states. The input to the model was lateral gust velocity and the output from the model consisted of three loads at the root of the vertical tail. MATRIX<sub>X</sub> SYSTEM BUILD<sup>10</sup> was used to construct the nonlinear simulation model.

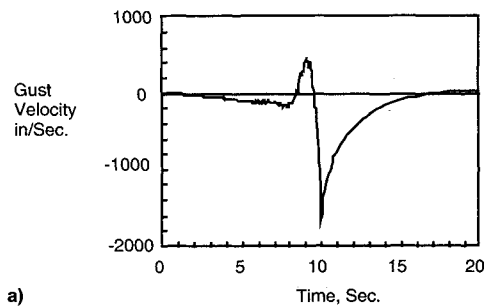
### Results and Discussion

This section describes numerical results obtained by applying the MFB and SSB methods to the linear and nonlinear models. For the particular nonlinear model chosen for this study, unrealistically large values of gust intensity had to be used in order to trigger the nonlinearities present in the system. For purposes of comparing results for linear and nonlinear models, the same large values of gust intensity were used for both.

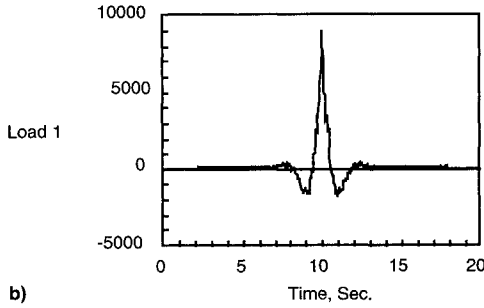
This section is in four parts. The first describes the calculations performed and presents the nomenclature that will be

Table 1 Calculations performed

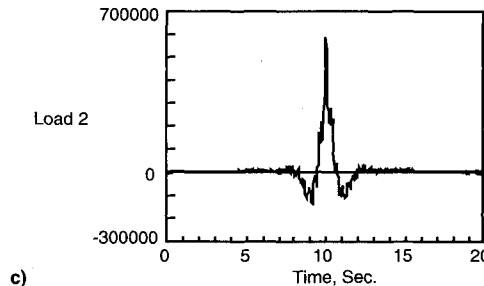
Model type	Matched-filter based			Stochastic-simulation based
	Linear	One dimensional	Multidimensional	
Linear	MFB-L $\sigma_g = 85$ ft/s $t_0 = 10$ s	—	—	SSB <sub>L</sub> $\sigma_g = 28.33$ ft/s $\tau_0 = 3, 6, 9, 12$ s $T = 450$ s
Nonlinear	—	MFB-1D $\sigma_g = 85, 170,$ $240, 255$ ft/s $t_0 = 10$ s	MFB-MD $\sigma_g = 85$ ft/s $t_0 = 10$ s	SSB <sub>N</sub> $\sigma_g = 28.33$ ft/s $\tau_0 = 6$ s $T = 450$ s



a)

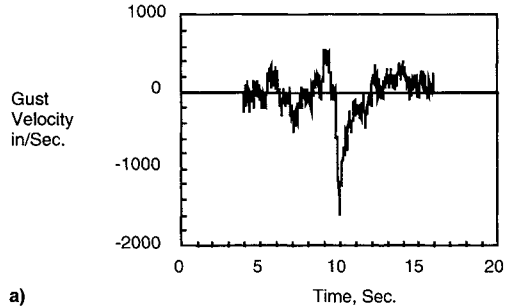


b)

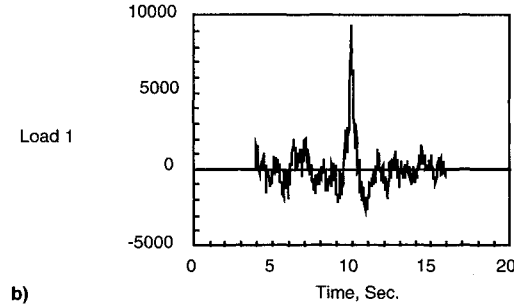


c)

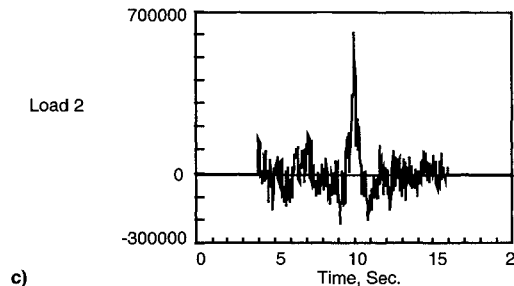
Fig. 7 Time histories of key quantities. MFB linear method and linear system.  $t_0 = 10$  s.  $\sigma_g = 240$  ft/s: a) critical gust profile, b) maximized load, and c) time-correlated load.



a)



b)



c)

Fig. 8 Time histories of key quantities. SSB method and linear system.  $t_0 = 6$  s.  $\sigma_g = 80$  ft/s: a) critical gust profile, b) maximized load, and c) time-correlated load.

used throughout this section. The second and third sections discuss the results for the linear and nonlinear models, respectively. The fourth section makes a comparison of the methods.

#### Summary of Analyses Performed

Table 1 contains a summary of the models used (linear or nonlinear), methods employed (MFB or SSB), and parameter values ( $\sigma_g$ ,  $t_0$ ,  $\tau_0$ , and  $T$ ).

For the SSB calculations the same white noise input was used in all the analyses. Also, the value of  $\eta_d$  was chosen to be 3, so that MFB and SSB analyses use gust intensities that differ by a factor of 3 as explained in the Selection of Gust Intensities section of this article.

The boldface titles in the various columns are to be used when discussing the various results. For example, when MFB-L is cited in the text it refers to the MFB linear analysis of the linear aircraft. MFB-1D refers to the one-dimensional search results for the nonlinear model.

#### Results Using the Linear Model

One of the intents of this article is to demonstrate, through the numerical results, that the MFB and SSB methods yield strikingly similar results. Figures 7 and 8 contain the MFB and SSB results for the linear model. In comparing the shapes of the corresponding time-history plots, it is apparent that the results are quite similar. In addition, the load 1 peak values are within 3.8% of each other.

The SSB<sub>L</sub> averaged-extracted peaks for load 1 are plotted as functions of  $\tau_0$  in Fig. 9. These averaged peaks have been normalized by the load 1 rms value and are represented by the dots in the figure. Vertical bars and brackets indicating the largest- and smallest-extracted-normalized peaks have also been provided. The largest-extracted peak is independent of  $\tau_0$  and is equal to the largest peak in the simulation. The smallest- and the averaged-extracted peaks generally increase with increasing  $\tau_0$  and approach the largest peak in the simulation record. Theoretically, the largest peak in the simulation increases with increasing total simulation length  $T$  as the probability of encountering higher and higher peaks increases. For small  $\tau_0$  values, many peaks near zero will enter the average, tending to reduce the averaged-peak value. Thus, by such variations of  $T$  and  $\tau_0$ , there appears to be some latitude in the range of averaged-extracted-peak value that can be obtained.

The data shown in Fig. 9 for  $\tau_0 = 6$  s, corresponds to the data presented in Fig. 8b. The value of the normalized-averaged-extracted peak is in the neighborhood of 3. This corresponds to the factor  $\eta_d$ , that was used in obtaining the SSB gust intensity, and serves to show why the results in Figs. 7 and 8 are very similar. As shown in Fig. 9, the normalized-averaged-extracted peak for  $\tau_0$  values other than 6 s differs from 3, indicating that the results for those  $\tau_0$  values would not be the same as the MFB answer.

#### Results Using the Nonlinear Model

The types of nonlinearities of most concern in determining aircraft design loads are control system nonlinearities. For

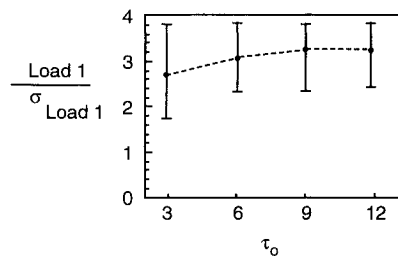


Fig. 9 Effect of  $\tau_0$  on load 1 results from SSB method. Linear system.  $\sigma_g = 80$  ft/s.

low-intensity disturbances, it can be expected that control system nonlinearities will have little effect on the load responses. Thus, the nonlinear response will be much like its linear counterpart. Consequently, any parameter that affects the disturbance level can be expected to have a threshold below which the system behaves linearly.

For the methods described in this article, two parameters affect disturbance intensity. A parameter common to all the analyses was the gust intensity  $\sigma_g$ . The other parameter was the impulse strength  $k$ , which is only used in the MFB one-dimensional search.

For clarity, the parts of this subsection are labeled according to the results discussed.

#### MFB-1D

Before the MFB-1D results are described and interpreted, a discussion of the general effect of the impulse strength and gust intensity on nonlinear systems is in order.

The variation of  $k$  affects the MFB-1D analysis by changing the shape of the excitation waveform. For sufficiently low impulse strengths, the shape of the excitation waveform for nonlinear models will be invariant with  $k$ . While in this invariant region, the excitation waveform will be the same as that obtained from the linear model. For larger intensities the system nonlinearities will cause the impulse responses and corresponding excitation waveforms to change shape. Consequently, they will no longer be the same as those obtained from the linear system.

The gust intensity affects the one-dimensional search by scaling the excitation waveform prior to being applied to the nonlinear model. Consequently, a low gust intensity should result in the nonlinear model behaving linearly. As gust intensity is increased beyond some threshold the nonlinear model

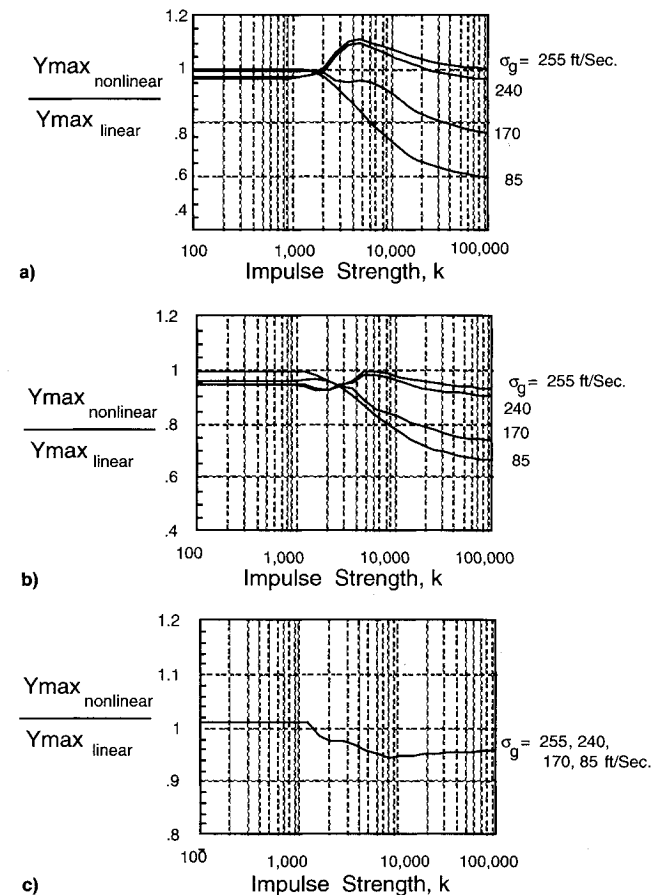


Fig. 10 Normalized maximum loads as functions of impulse strength. MFB one-dimensional method.  $t_0 = 10$  s. Loads a) 1, b) 2, and c) 3.

response will begin to deviate from that of its linear counterpart.

One-dimensional search results were obtained at the four gust intensities shown in the part labeled MFB-1D in Table 1. Figure 10 shows the results for each of the three loads. Each part of Fig. 10 contains plots of normalized maximized load as functions of impulse strength: part a) presents the results for maximizing load 1, part b) for maximizing load 2, and part c) for maximizing load 3. The normalizing quantity for each load at each value of  $\sigma_g$  is the value of  $y_{\max}$  obtained from a corresponding MFB linear analysis of the linear model.

With the preceding discussion in mind the results shown in Fig. 10 will be interpreted, beginning with load 1. The shape of the excitation waveform is invariant for values of  $k$  below 1000. As a result, the peak loads are invariant with  $k$  for

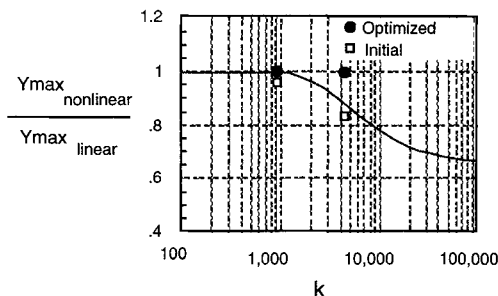


Fig. 11 Normalized maximum loads for load 2. MFB multidimensional method.  $t_0 = 10$  s.  $\sigma_g = 240$  ft/s.

impulse strengths less than this threshold at all the gust intensities.

At the lowest gust intensity (85 ft/s) the largest load obtained from the analysis is obtained at the low values of  $k$ . In addition, the ratio of  $y_{\max}$  nonlinear to  $y_{\max}$  linear is unity for these low  $k$  values. This indicates that the nonlinear model behaves linearly for load 1 at this gust intensity.

At sufficiently large gust intensities the peak value of load 1 occurs at an impulse strength greater than 1000, with a ratio of  $y_{\max}$  nonlinear to  $y_{\max}$  linear being larger than in the invariant region. This indicates that the nonlinearity has a significant effect on the load, and is of great importance at this gust intensity.

Similar trends are noted for load 2 in Fig. 10. Load 3, on the other hand, is invariant with gust intensity, and the largest load is obtained for low values of  $k$ . This indicates that the nonlinear control system has very little effect on load 3 at all the gust intensities investigated.

#### MFB-MD

Two separate multidimensional searches were performed on the nonlinear transport model to maximize load 2 at a gust intensity of 85 ft/s. The number of design variables used in the optimization procedure was 160. Reference 4 gives a detailed description of what the design variables represent and how to select the proper number to use.

These MFB-MD results are shown plotted in Fig. 11 with the corresponding MFB-1D curve from Fig. 10b. While the value of  $k$  has no bearing on the multidimensional result, the location of each of the two sets of starting and ending points with respect to the  $k$  axis indicates the value that was used

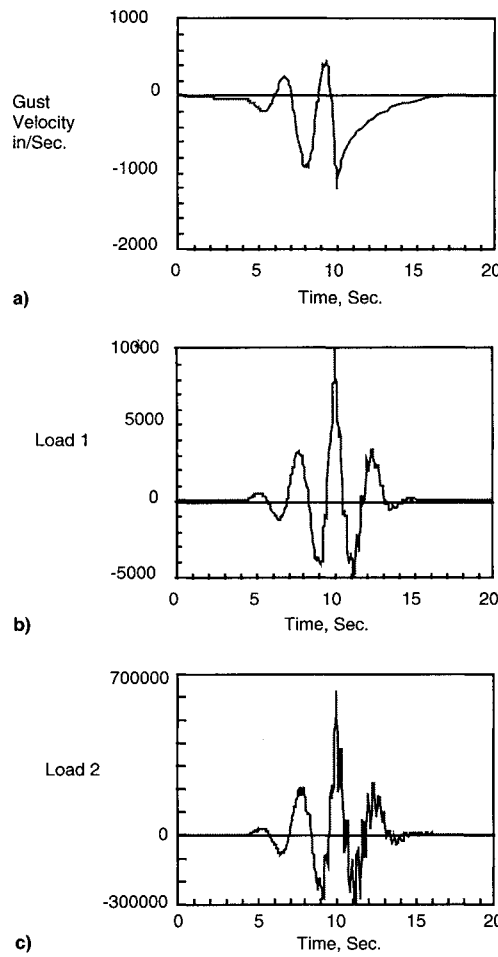


Fig. 12 Time histories of key quantities. MFB one-dimensional method and nonlinear system.  $t_0 = 10$  s.  $\sigma_g = 240$  ft/s: a) critical gust profile, b) maximized load, and c) time-correlated load.

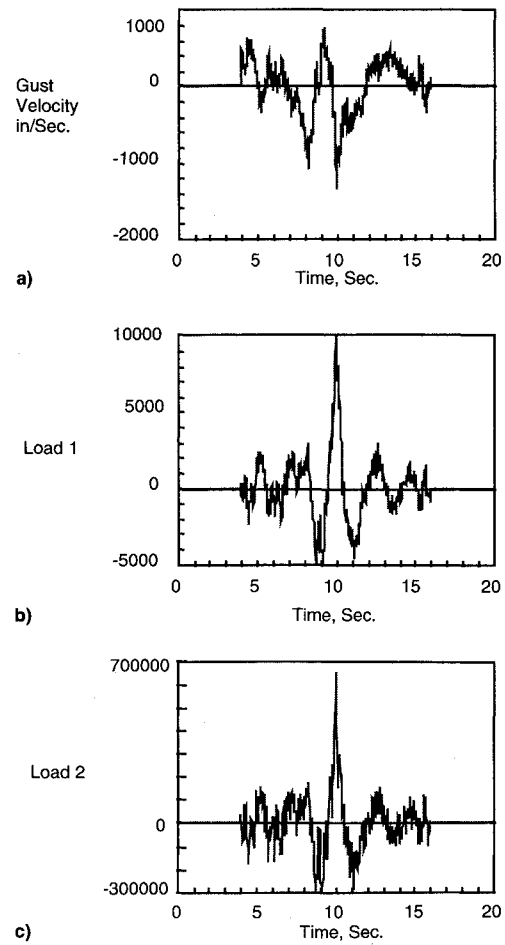


Fig. 13 Time histories of key quantities. SSB method and nonlinear system.  $t_0 = 6$  s.  $\sigma_g = 80$  ft/s: a) critical gust profile, b) maximized load, and c) time-correlated load.

Table 2 Comparison of simulation time required

Model type	Matched-filter based			Stochastic-simulation based
	Linear	One dimensional	Multidimensional	
Linear	60 s	—	—	450 s
Nonlinear	—	300 s	10,800 s	450 s

to generate the starting excitation waveform for the search. The first search used, as the initial condition, the critical gust profile corresponding to an impulse strength of 900; the other used the critical gust profile corresponding to an impulse strength of 4300. The initial conditions are depicted in the figure by open symbols; the optimized results, by closed symbols.

The MFB-MD results indicate that, for this particular load and gust intensity, the multidimensional search increased the maximum value of load 2 no more than the highest value achieved by the one-dimensional search. In this instance, then, the one-dimensional search was sufficient to provide the maximized load.

#### Comparison of MFB-1D and SSB<sub>N</sub>

Again, keeping in mind that one of the intents of this article is to demonstrate that the MFB and SSB methods yield similar results, a comparison can be made of the nonlinear time histories. Figures 12 and 13 contain the MFB-1D and SSB<sub>N</sub> results, respectively. These analyses were performed with  $U_{\sigma} = 240$  ft/s. As with the analogous linear results, the time-history plots obtained using the MFB-1D and SSB<sub>N</sub> calculations for the nonlinear model are quite similar in shape and peak load value. Thus, the one-dimensional search obtained the worst-case gust profile for the nonlinear model without the need for MFB multidimensional search.

By comparing the linear results in Figs. 7 and 8 with the nonlinear results in Figs. 12 and 13, a significant difference is noted between the linear results and the nonlinear results. This observation indicates that there is a substantial difference between the linear and nonlinear response at this  $U_{\sigma}$  value. This indicates the need for using methods capable of handling the nonlinearities. This result is also consistent with the one-dimensional search prediction that the nonlinearities would significantly affect aircraft response at this  $U_{\sigma}$  value. These observations suggest that the MFB one-dimensional search is capable of effectively locating the worst-case gust profile and corresponding maximized load.

#### Comparison of SSB<sub>N</sub> and SSB<sub>L</sub>

To further explore the effect of gust intensity on the response of the nonlinear aircraft, the normalized load level exceedances were extracted from the SSB linear and nonlinear analyses time histories. Figure 14 shows the level crossing results of both the SSB<sub>N</sub> and SSB<sub>L</sub> analyses for each of the three loads. For each load, the solid line represents the theoretical level-crossing curve predicted by Rice's equation.<sup>7</sup> The symbols represent the number of crossings of various load levels. The load levels have been normalized by corresponding  $\sigma_g$  values.

Figure 14 shows the linear results and the nonlinear results at the lower gust intensity (28.33 ft/s) to be essentially the same. This is consistent with the one-dimensional search prediction where the largest load was obtained in the invariant region, indicating linear behavior of the nonlinear model.

The load 1 and load 2 linear results and the nonlinear results at the larger gust intensity (80 ft/s) differ significantly at large load levels. Again, these results are consistent with the one-dimensional search prediction where the largest loads obtained for loads 1 and 2 did not occur in the invariant region, thus indicating the importance of the nonlinearity.

Figure 14c shows the load 3 linear results and the nonlinear results at all the gust intensities to be quite similar. This is

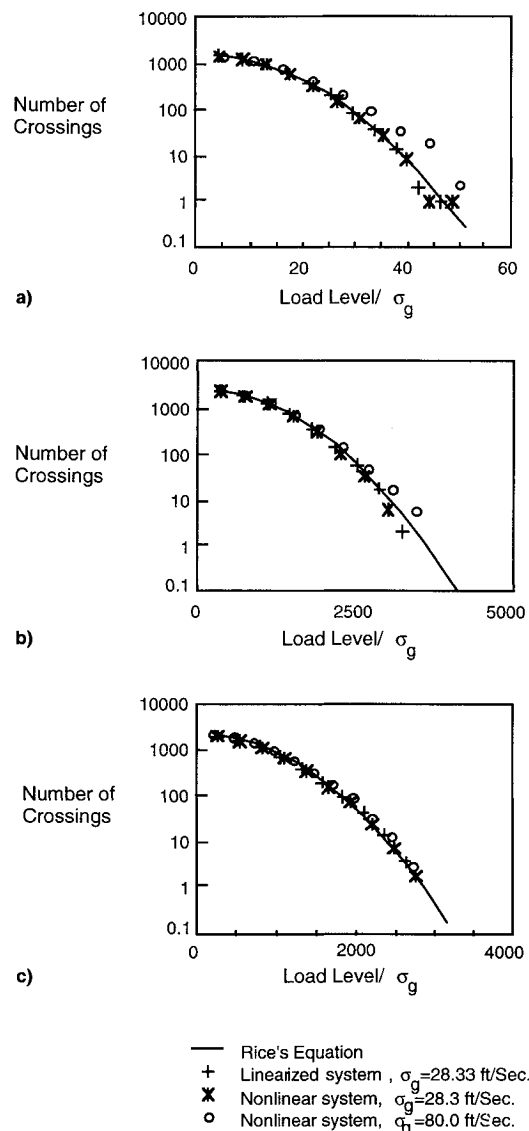


Fig. 14 Number load level crossing from SSB method. Loads a) 1, b) 2, and c) 3.

consistent with the one-dimensional search prediction where the largest load was obtained in the invariant region and the nonlinearity had little effect on this load.

#### Comparison of Efficiencies of the MFB and SSB Methods

Two measures may be used to compare the efficiency of the MFB and SSB methods. One is the amount of computer storage required, and the other is the amount of CPU time required to perform the calculations. The SSB method required approximately 25 times more storage than the MFB methods, and Table 2 shows a comparison of the approximate total seconds of simulation required to perform a complete analysis for this model at one gust intensity.

For the linear model, the MFB method is more efficient than the SSB method. For nonlinear systems the MFB mul-

tidimensional search is much more expensive than the SSB method, while the MFB one-dimensional search requires less time than the SSB method. The SSB method requires the same amount of simulation time for both linear and nonlinear models.

Since the multidimensional search is prohibitively expensive, the practical options for methods applicable to nonlinear systems are the MFB one-dimensional search and the SSB method. Based on the preceding discussion, the one-dimensional search is able to predict the maximized loads for nonlinear systems. In addition, it requires less computer resources than the SSB method. These factors point to the MFB one-dimensional search as a means of replacing or at least complementing stochastic approaches.

### Concluding Remarks

This article has described two analysis methods, one deterministic and the other stochastic, for computing maximized and time-correlated gust loads for aircraft with nonlinear control systems. The MFB and SSB methods were applied to a mathematical model of a current transport aircraft equipped with a nonlinear yaw damper.

The results predicted by the two methods are strikingly similar and demonstrate that the key quantities from the MFB method (viz., critical gust profile, maximized load, and time-correlated load) are realizable in the SSB method. Another significant finding is the relative computational costs of performing analyses using the MFB and SSB methods. Based on the total amount of simulation time required to obtain maximized and time-correlated loads, the SSB method costs about one and a half times as much as the MFB one-dimensional search. The cost for the MFB multidimensional search is about one and a half orders of mag-

nitude more than the cost of the MFB one-dimensional search.

### References

- <sup>1</sup>Perry, B., III, Pototzky, A. S., and Woods, J. A., "NASA Investigation of a Claimed "Overlap" Between Two Gust Response Analysis Methods," *Journal of Aircraft*, Vol. 27, No. 7, 1990, pp. 605-611.
- <sup>2</sup>Pototzky, A. S., Zeiler, T. A., and Perry, B., III, "Calculating Time-Correlated Gust Loads Using Matched Filter and Random Process Theories," *Journal of Aircraft*, Vol. 28, No. 5, 1991, pp. 346-352.
- <sup>3</sup>Zeiler, T. A., and Pototzky, A. S., "On the Relationship Between Matched Filter Theory as Applied to Gust Loads and Phased Design Loads Analysis," NASA CR-181802, April 1989.
- <sup>4</sup>Scott, R. C., Pototzky, A. S., and Perry, B., III, "Computation of Maximized Gust Loads for Nonlinear Aircraft Using Matched-Filter-Based Schemes," *Journal of Aircraft*, Vol. 30, No. 5, 1993, pp. 763-768.
- <sup>5</sup>Scott, R. C., Pototzky, A. S., and Perry, B., III, "Determining Design Gust Loads for Nonlinear Aircraft—Similarity Between Methods Based on Matched Filter Theory and on Stochastic Simulation," NASA TM-107614, April 1992.
- <sup>6</sup>Barr, N. M., Gangsaas, D., and Schaeffer, D. R., "Wind Tunnel Models for Flight Simulator Certification of Landing and Approach Guidance and Control Systems," Boeing Commercial Airplane Co., Final Rept. FAA-RD-74-206, Seattle, WA, Dec. 1974.
- <sup>7</sup>Hoblit, F. M., *Gust Loads on Aircraft: Concepts and Applications*, 1st ed., AIAA Education Series, AIAA, Washington, DC, 1988.
- <sup>8</sup>Gould, J. D., "Effects of Active Control System Nonlinearities on the L-1011-3(ACS) Design Gust Loads," AIAA Paper 85-0755, April 1985.
- <sup>9</sup>Richardson, J. R., "A More Realistic Method for Routine Flutter Calculations," *AIAA Symposium on Structural Dynamics and Aeroelasticity*, AIAA, New York, 1965, pp. 10-17.
- <sup>10</sup>Anon., "SYSTEM\_BUILD 7.0 User's Guide," Integrated Systems Inc., Santa Clara, CA, Oct. 1988.